

# Theory of Neutrino Masses and Mixing \*

M. C. Gonzalez-Garcia <sup>a</sup>

CERN-TH/2002-295  
YITP-SB-02-52  
IFIC/02-49  
hep-ph/yymmddd

<sup>a</sup>Theory Division, CERN, CH-1211, Geneva 23, Switzerland,  
Y.I.T.P., SUNY at Stony Brook, Stony Brook, NY 11794-3840  
and IFIC, Universitat de València – C.S.I.C., Apt 22085, 46071 València, Spain

In this talk I will review our present knowledge on neutrino masses and mixing trying to emphasize what has been definitively proved and what is in the process of being probed. I will also discuss the most important theoretical implications of these results: the existence of new physics, the estimate of the scale of this new physics as well as some other possible consequences such as leptogenesis origin of the baryon asymmetry.

## 1. Introduction

Neutrino physics is a very exciting field at this moment. From the plenary talk by D. Wark [1] as well as from the talks by S. Oser [2], M.R. Vagins [3], T. Mitsui [4], C. Mauger [5], Y. Hayato [6], Y. Itow [7], A. Bazarko [8] and J. Urheim [9] in the neutrino parallel session we have heard about the enormous progress made and being made in the experimental front from which we have learned that

- Solar  $\nu'_e$ 's convert to  $\nu_\mu$  or  $\nu_\tau$ . This evidence was first established at  $3.4\sigma$  by the comparison of the SNO results [2] on the charged current (CC) measurement with the results from SuperKamiokande(SK) on the electron scattering (ES) [3] of  $^8\text{B}$  neutrinos, and with more than  $5\sigma$  from the subsequent SNO neutral current (NC) and CC observations [2]. These results are new since the last ICHEP conference in Osaka.
- The evidence of atmospheric  $\nu_\mu$  disappearing from SK is now at  $> 15\sigma$ , most likely converting to  $\nu_\tau$  [5]. K2K data [6] supports within statistics the disappearance of  $\nu_\mu$ 's. The most likely explanation is neutrino oscillations.

\*Plenary talk given at the 31st International Conference on High Energy Physics, ICHEP02 (Amsterdam, 24-31 July, 2002).

- LSND found evidence for  $\overline{\nu_\mu} \rightarrow \overline{\nu_e}$  which is being tested by MiniBooNE [8].

The experimental results have triggered a very intense activity in the phenomenological and theoretical front. In Fig. 1 I show the number of papers in SPIRES with the word “neutrino” in the title as a function of the year where one can see the clear *forward peak* corresponding to the last two years since the last ICHEP conference. This figure makes it clear that it is impossible to summarize in full fairness the activity of the field. I will concentrate on reviewing the phenomenological interpretations and some of the theoretical implications of the experimental results.

The outline of the talk is as follows: in Sec. 1.1 I will briefly review the notation and parameter space of neutrino oscillations. In Sec. 2 I will discuss the phenomenological interpretation of solar, atmospheric and laboratory experiments in terms of neutrino masses and mixing emphasizing the still-existing ambiguities and uncertainties in the interpretation. Sec. 3 is devoted to some of the theoretical implications. Finally in Sec. 4 I will discuss what we will learn in the near future from existing experiments and what will be still left to learn at proposed facilities.

### 1.1. Leptonic Mixing and $\nu$ Oscillations

If neutrinos have masses, flavour is mixed in the CC interactions of the leptons, and a leptonic mixing matrix will appear analogous to the

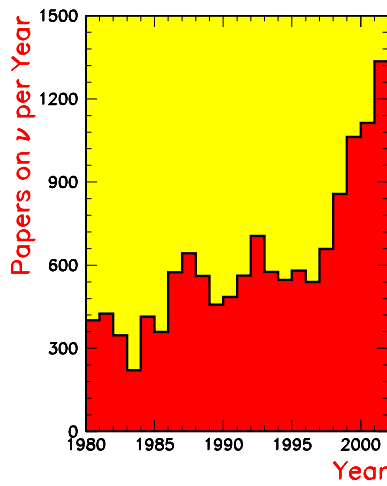


Figure 1. Number of papers in SPIRES with the word “neutrino” in the title as a function of the year.

CKM [11] matrix for the quarks. The possibility of arbitrary mixing between two massive neutrino states was first introduced in Ref. [10]. The discussion of leptonic mixing in generic models is complicated by two factors. First the number massive neutrinos ( $n$ ) is unknown, since there are no constraints on the number of right-handed, SM-singlet, neutrinos ( $m = n - 3$ ). Second, since neutrinos carry neither color nor electromagnetic charge, they could be Majorana fermions. Denoting the neutrino mass eigenstates by  $\nu_i$ ,  $i = 1, 2, \dots, n$ , and the charged lepton mass eigenstates by  $(e, \mu, \tau)$ , in the mass basis, leptonic charged current interactions are given by

$$-\mathcal{L}_{CC} = \frac{g}{\sqrt{2}} (\overline{e}_L \overline{\mu}_L \overline{\tau}_L) \gamma^\mu U \begin{pmatrix} \nu_1 \\ \vdots \\ \nu_n \end{pmatrix} W_\mu^+ + \text{h.c.} \quad (1)$$

Here  $U$  is a  $3 \times n$  matrix.

Given the charged lepton mass matrix  $M_\ell$  and the neutrino mass matrix  $M_\nu$  in some interaction basis [the interaction eigenstates are denoted by

$(e^I, \mu^I, \tau^I)$  and  $\vec{\nu} = (\nu_{Le}, \nu_{L\mu}, \nu_{L\tau}, \nu_{s1}, \dots, \nu_{sm})$ ]

$$-\mathcal{L}_M = (\overline{e}_L^I \overline{\mu}_L^I \overline{\tau}_L^I) M_\ell \begin{pmatrix} e_R^I \\ \mu_R^I \\ \tau_R^I \end{pmatrix} + \frac{1}{2} \overline{\nu^c} M_\nu \vec{\nu} + \text{h.c.}, \quad (2)$$

we can find the diagonalizing matrices  $V^\ell$  ( $3 \times 3$ ) and  $V^\nu$  ( $n \times n$ ):

$$\begin{aligned} V^{\ell\dagger} M_\ell M_\ell^\dagger V^\ell &= \text{diag}(m_e^2, m_\mu^2, m_\tau^2), \\ V^{\nu\dagger} M_\nu M_\nu^\dagger V^\nu &= \text{diag}(m_1^2, m_2^2, m_3^2, \dots, m_n^2) \end{aligned} \quad (3)$$

The  $3 \times n$  mixing matrix  $U$  can be found from these diagonalizing matrices:

$$U_{ij} = P_{\ell,ii} V_{ik}^\ell V_{kj}^\nu (P_{\nu,jj}). \quad (4)$$

$P_\ell$  is a diagonal  $3 \times 3$  phase matrix, that is conventionally used to reduce by three the number of phases in  $U$ .  $P_\nu$  is a diagonal matrix with additional arbitrary phases (chosen to reduce the number of phases in  $U$ ) only for Dirac states. For Majorana neutrinos, this matrix is simply a unit matrix. The reason for that is that if one rotates a Majorana neutrino by a phase, this phase will appear in its mass term which will no longer be real. Thus, the number of phases that can be absorbed by redefining the mass eigenstates depends on whether the neutrinos are Dirac or Majorana particles. In particular, if there are only three Majorana (Dirac) neutrinos,  $U$  is a  $3 \times 3$  matrix analogous to the CKM matrix for the quarks but due to the Majorana (Dirac) nature of the neutrinos it depends on six (four) independent parameters: three mixing angles and three (one) phases.

If no new interactions for the charged leptons are present we can identify their interaction eigenstates with the corresponding mass eigenstates after phase redefinitions. In this case the charged current lepton mixing matrix  $U$  is simply given by a  $3 \times n$  sub-matrix of the unitary matrix  $V^\nu$ .

The presence of the leptonic mixing, allows for flavour oscillations of the neutrinos. A neutrino of energy  $E$  produced in a CC interaction with a charged lepton  $l_\alpha$  can be detected via a CC interaction with a charged lepton  $l_\beta$  with a probability

$$P_{\alpha\beta} = \delta_{\alpha\beta} - 4 \sum_{i < j}^n \text{Re}[U_{\alpha i} U_{\beta i}^* U_{\alpha j}^* U_{\beta j}] \sin^2 x_{ij}$$

$$+2 \sum_{i < j}^n \text{Im}[U_{\alpha i} U_{\beta i}^* U_{\alpha j}^* U_{\beta j}] \sin^2 \frac{x_{ij}}{2}, \quad (5)$$

where in the convenient units:

$$x_{ij} = 1.27 \frac{\Delta m_{ij}^2}{\text{eV}^2} \frac{L/E}{\text{m/MeV}}. \quad (6)$$

with  $\Delta m_{ij}^2 \equiv m_i^2 - m_j^2$ .  $L = t$  is the distance between the production point of  $\nu_\alpha$  and the detection point of  $\nu_\beta$ . The first line in Eq. (5) is CP conserving while the second one is CP violating and has opposite sign for  $\nu$  and  $\bar{\nu}$ .

The transition probability [Eq. (5)] presents an oscillatory behaviour, with oscillation lengths  $L_{0,ij}^{\text{osc}} = \frac{4\pi E}{\Delta m_{ij}^2}$  and amplitude that is proportional to elements in the mixing matrix. From Eq. (5) we find that neutrino oscillations are only sensitive to mass squared differences. Also, the Majorana phases cancel out and only the Dirac phase is observable in the CP violating term. In order to be sensitive to a given value of  $\Delta m_{ij}^2$ , an experiment has to be set up with  $E/L \approx \Delta m_{ij}^2$  ( $L \sim L_{0,ij}^{\text{osc}}$ ).

For a two-neutrino case, the mixing matrix depends on a single parameter, there is a single mass-squared difference  $\Delta m^2$  and there is no Dirac CP phase. Then  $P_{\alpha\beta}$  of Eq. (5) takes the well known form

$$P_{\alpha\beta} = \delta_{\alpha\beta} - (2\delta_{\alpha\beta} - 1) \sin^2 2\theta \sin^2 x. \quad (7)$$

The full physical parameter space is covered with  $\Delta m^2 \geq 0$  and  $0 \leq \theta \leq \frac{\pi}{2}$  (or, alternatively,  $0 \leq \theta \leq \frac{\pi}{4}$  and either sign for  $\Delta m^2$ ). Changing the sign of the mass difference,  $\Delta m^2 \rightarrow -\Delta m^2$ , and changing the octant of the mixing angle,  $\theta \rightarrow \frac{\pi}{2} - \theta$ , amounts to redefining the mass eigenstates,  $\nu_1 \leftrightarrow \nu_2$ :  $P_{\alpha\beta}$  must be invariant under such transformation. Eq. (7) reveals, however, that  $P_{\alpha\beta}$  is actually invariant under each of these transformations separately. This situation implies that there is a two-fold discrete ambiguity in the interpretation of  $P_{\alpha\beta}$  in terms of two-neutrino mixing: the two different sets of physical parameters,  $(\Delta m^2, \theta)$  and  $(\Delta m^2, \frac{\pi}{2} - \theta)$ , give the same transition probability in vacuum. One cannot tell from a measurement of, say,  $P_{e\mu}$  in vacuum whether the larger component of  $\nu_e$  resides in the heavier or in the lighter neutrino mass eigenstate.

This symmetry is lost when neutrinos travel through regions of dense matter. In this case, they can undergo forward scattering with the particles in the medium. These interactions are, in general, flavour dependent and they can be included as a potential term in the evolution equation of the flavour states. As a consequence the oscillation pattern is modified. Let us consider, for instance, oscillations  $\nu_e \rightarrow \nu_\mu$  in a neutral medium like the Sun or the Earth. For this system, the instantaneous mixing angle in matter takes the form

$$\sin 2\theta_m = \frac{\Delta m^2 \sin 2\theta}{\sqrt{(\Delta m^2 \cos 2\theta - A)^2 + (\Delta m^2 \sin 2\theta)^2}} \quad (8)$$

where  $A = 2EV_{\text{CC}} = 2\sqrt{2}EG_F N_e$  ( $N_e$  is the electron number density in the medium). Eq (8) shows an enhancement (reduction) of the mixing angle in matter for  $\theta < \frac{\pi}{4}$  ( $\theta > \frac{\pi}{4}$ ) [12]. Thus, matter effects allow to determine whether the larger component of  $\nu_e$  resides in the lighter neutrino mass eigenstate. As we will see this is the presently favoured scenario for solar neutrino oscillations. For mixing of three or more neutrinos, the oscillation probability, even in vacuum, does not depend in general of  $\sin^2 2\theta_{ij}$ .

Neutrino oscillation experiments measure  $P_{\alpha\beta}$ . It is common practice to interpret these results in the two-neutrino framework and translate the constraints on  $P_{\alpha\beta}$  into allowed or excluded regions in the plane  $(\Delta m^2, \sin^2 2\theta)$ . However, as we have seen once matter effects are important, or mixing among more than two neutrinos is considered, the covering of the full parameter space requires the use of a single-valued function of the mixing angle such as  $\sin^2 \theta$  or  $\tan^2 \theta$  [13].

## 2. Global Fits

### 2.1. Solar Neutrinos

The sun is a source of  $\nu'_e$ s which are produced in the different nuclear reactions taking place in its interior. Along this talk I will use the  $\nu_e$  fluxes from Bahcall–Pinsonneault calculations [14] which I refer to as the solar standard model (SSM). These neutrinos have been detected at the Earth by seven experiments which use different detection techniques [1]. Due to the

Experiment	Detection	Flavour	$E_{\text{th}}$ (MeV)	$\frac{\text{Data}}{\text{BP00}}$
Homestake	$^{37}\text{Cl}(\nu, e^-)^{37}\text{Ar}$	$\nu_e$	$E_{\nu} > 0.81$	$0.34 \pm 0.03$
Sage + Gallex+GNO	$^{71}\text{Ga}(\nu, e^-)^{71}\text{Ge}$	$\nu_e$	$E_{\nu} > 0.23$	$0.56 \pm 0.04$
Kam $\Rightarrow$ SK	ES $\nu_x e^- \rightarrow \nu_x e^-$	$\nu_e, \nu_{\mu/\tau}$ $(\frac{\sigma_{\mu\tau}}{\sigma_e} \simeq \frac{1}{6})$	$E_e > 5$	$0.46 \pm 0.02$
SNO	CC $\nu_e d \rightarrow p p e^-$ NC $\nu_x d \rightarrow \nu_x d$ ES $\nu_x e^- \rightarrow \nu_x e^-$	$\nu_e$ $\nu_e, \nu_{\mu/\tau}$ $\nu_e, \nu_{\mu/\tau}$	$T_e > 5$ $T_{\gamma} > 5$ $T_e > 5$	$0.35 \pm 0.02$ $1.01 \pm 0.12$ $0.47 \pm 0.05$

Table 1

Event rates observed at solar neutrino experiments compared to the SSM predictions (the errors do not include the theoretical uncertainties). For SNO, the quoted rates are obtained under the hypothesis of undistorted  $^8\text{B}$  spectrum.

different energy threshold and the different detection reactions, the experiments are sensitive to different parts of the solar neutrino spectrum and to the flavour composition of the beam. In table 2.1 I show the different experiments and detection reactions with their energy threshold as well as their latest results on the total event rates as compared to the SSM prediction. We can make the following statements:

- Before the NC measurement at SNO all experiments observed a flux that was smaller than the SSM predictions,  $\Phi^{\text{obs}}/\Phi^{\text{SSM}} \sim 0.3 - 0.6$ .
- The deficit is not the same for the various experiments, which indicates that the effect is energy dependent.
- SNO has observed an event rate different in the different reactions. In particular in NC SNO observed no deficit as compared to the SSM.

The first two statements constitute the solar neutrino problem. The last one, has provided us in the last year with evidence of flavour conversion of solar neutrinos independent of the solar model.

Both SK and SNO measure the high energy  $^8\text{B}$  neutrinos. Schematically, in presence of flavour conversion the observed fluxes in the different reactions are

$$\Phi^{\text{CC}} = \Phi_e,$$

$$\begin{aligned} \Phi^{\text{ES}} &= \Phi_e + r \Phi_{\mu\tau}, \\ \Phi^{\text{NC}} &= \Phi_e + \Phi_{\mu\tau}, \end{aligned} \quad (9)$$

where  $r \equiv \sigma_{\mu}/\sigma_e \simeq 0.15$  is the ratio of the the  $\nu_e - e$  and  $\nu_{\mu} - e$  elastic scattering cross-sections. The flux  $\Phi_{\mu\tau}$  of active no-electron neutrinos is zero in the SSM. Thus, in the absence of flavour conversion, the three observed rates should be equal. The first reported SNO CC result compared with the ES rate from SK showed that the hypothesis of no flavour conversion was excluded at  $\sim 3\sigma$ . Finally, with the NC measurement at SNO one finds that

$$\Phi_{\mu\tau} = (3.41 \pm 0.45^{+0.48}_{-0.45}) \times 10^6 \text{ cm}^{-2}\text{s}^{-1}. \quad (10)$$

This result provides evidence for neutrino flavor transition (from  $\nu_e$  to  $\nu_{\mu,\tau}$ ) at the level of  $5.3\sigma$ . This evidence is independent of the solar model.

The most generic and popular explanation to this observation is in terms of neutrino masses and mixing leading to oscillations of  $\nu_e$  into an active ( $\nu_{\mu}$  and/or  $\nu_{\tau}$ ) or a sterile ( $\nu_s$ ) neutrino. Several global analyses of the solar neutrino data have appeared in the literature after the latest SNO results [15]. In Fig. 2 I show the results of a global analysis [16] of the latest solar neutrino data in terms of oscillation parameters.

To illustrate the progress in the last two years, I show in the same figure the allowed parameter space which I showed in my talk at the ICHEP00 conference two years ago [17]. The progress can be summarized as follows:

- Two years ago for the case of active-active neutrino oscillations we found three allowed regions for the global fit: the SMA solution, the LMA and LOW-QVO solution. The best solution was LMA but the other solutions were there at 95% CL. At 99% CL the LMA region extended beyond maximal mixing and to  $\Delta m^2$  above  $10^{-3}$  eV<sup>2</sup>. For sterile neutrinos the fit was slightly worse (due to the lack of neutral current contribution to SK) but still reasonable.
- At present we find that active oscillations are clearly favoured. LMA is the best fit and the only solution at  $\sim 99\%$  CL. At  $3\sigma$  the allowed parameter space within LMA is in the first octant and there is an upper bound  $\Delta m^2 \leq 4 \times 10^{-4}$  eV<sup>2</sup>. SMA is ruled out at  $\sim 4\sigma$  as a consequence of the tension between the low rate observed by SNO in CC and the flat spectrum observed by SK. Sterile oscillations are disfavoured at  $\sim 5\sigma$  due to the difference between the observed CC and NC event rates at SNO.

In making this progress both the more detailed information on the day-night spectrum of SK and the new SNO results have played very important and complementary roles.

Next we can ask ourselves how certain we are that the flavour conversion mechanism for solar neutrinos is indeed oscillations. To answer this question we can study which information we have on the actual energy dependence of the flavour conversion probability from the solar neutrino data in a model independent way [18]. To do so one can fit the observed rates assuming different average survival probabilities in three different energy ranges of the solar neutrinos: low energy neutrinos, whose largest flux is the  $pp$  flux, with survival probability  $\langle P_{ee} \rangle_L$ , a region of intermediate energy, consisting of the  $^7B$ ,  $pep$  and CNO fluxes, with survival probability  $\langle P_{ee} \rangle_I$ , and the higher energy part, whose dominant contribution is due to  $^8B$  neutrinos, with survival probability  $\langle P_{ee} \rangle_H$ . I show the results of this exercise in Fig. 3 together with the predicted energy dependence of the survival probability at the best fit point of LMA and LOW oscillations as well as

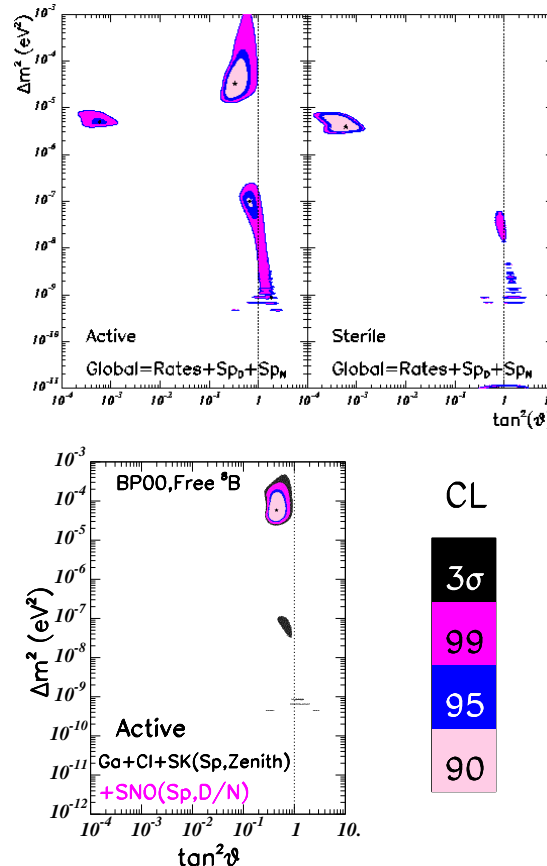


Figure 2. Allowed regions from the global fit for solar neutrino oscillations. The upper panels show the status at the time of the ICHEP00 conference and the lower panel gives the results from the last updated analysis in Ref. [16].

for other alternative scenarios of solar neutrino flavour conversion.

While the LMA oscillation may provide the simplest explanation of the data, there are presently alternative scenarios which fit the data equally well. For example spin-flavor precession [19] in which the neutrinos have an anomalous transition magnetic moment, which allows them to interact coherently with the magnetic field in the Sun. This can lead to resonant as well as non-resonant (RSFP and NRSFP respectively in Fig. 3) flavour transitions of neutrinos into anti-neutrinos which, as seen in the fig-

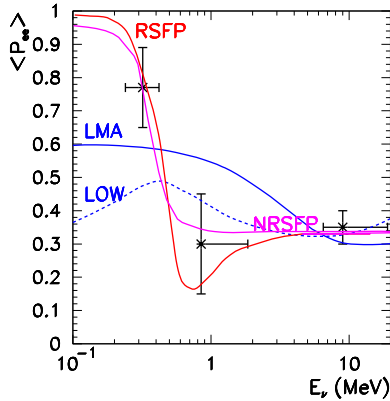


Figure 3. Reconstructed values of the survival probability of solar neutrinos in different energy ranges from a fit to the observed rates, together with the predictions from different flavour conversion mechanisms.

ure can describe the observations (for appropriate choice of the magnetic field configuration), but implying masses and mixing different than oscillations [20]. For instance, for the case of RSFP the analysis of the data gives values of  $\Delta m^2 = (0.8 - 1.5) \cdot 10^{-8} \text{ eV}^2$ .

Even for massless neutrinos, the mixing and level splitting required for neutrino flavour conversion can be induced by flavour changing neutrino interaction with matter [21].

This alternative scenarios can be considered not very attractive from the theoretical point of view, since they require some of the corresponding additional parameters (magnetic moments and flavour changing couplings in the cases mentioned above) to take “unnaturally” (although still experimentally allowed) large values. However, as I will discuss in Sec. 4 we are in the privileged situation that our theoretical prejudices will soon become irrelevant since we have a running experiment, KamLAND which, if it observes an oscillation signal, will rule out these scenarios as the main mechanism of solar flavour conversion.

## 2.2. Atmospheric Neutrinos

Atmospheric showers are initiated when primary cosmic rays hit the Earth’s atmosphere.

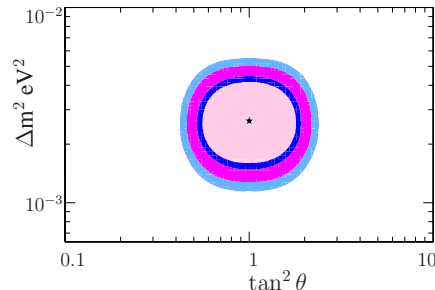


Figure 4. Allowed parameters from the global fit of atmospheric neutrino data for  $\nu_\mu \rightarrow \nu_\tau$  oscillations from Ref. [23].

Secondary mesons produced in this collision, mostly pions and kaons, decay and give rise to electron and muon neutrino and anti-neutrinos fluxes whose interactions are detected in underground detectors [1,5].

At present the atmospheric neutrino anomaly (ANA) can be summarized in three observations:

- There has been a long-standing deficit of about 60 % between the predicted and observed  $\nu_\mu/\nu_e$  ratio of the contained events strengthened by the high statistics sample collected at the SK experiment.
- The most important feature of the atmospheric neutrino data at SK is that it exhibits a *zenith-angle-dependent* deficit of muon neutrinos which indicates that the deficit is larger for muon neutrinos coming from below the horizon which have traveled longer distances before reaching the detector. On the contrary, electron neutrinos behave as expected in the SM.
- The deficit for through-going muons is smaller than for stopping muons, *i.e.* the deficit decreases as the neutrino energy grows.

The most likely solution of the ANA involves neutrino oscillations. At present the best solution from a global analysis of the atmospheric neutrino data is  $\nu_\mu \rightarrow \nu_\tau$  oscillations with oscillation parameters shown in Fig. 4

Oscillations into electron neutrinos are nowadays ruled out since they cannot describe the measured angular dependence of muon-like contained events. Moreover the most favoured range

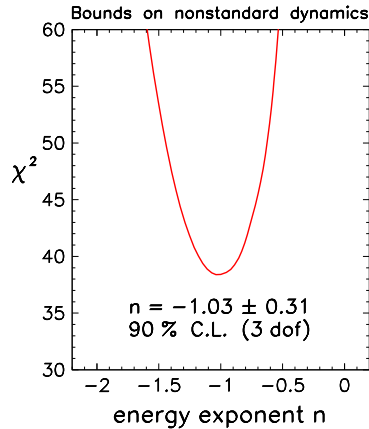


Figure 5. Results of a phenomenological fit of various flavour conversion mechanism to the atmospheric neutrino data Ref. [24].

of masses and mixings for this channel have been excluded by the negative results from the CHOOZ reactor experiment [25]. Oscillations into sterile neutrinos are also disfavoured because due to matter effects in the Earth they predict a flatter-than-observed angular dependence of the through-going muon data [5].

Again, we can ask ourselves how certain we are that the flavour conversion mechanism for atmospheric neutrinos is indeed oscillations. The answer is that the case for atmospheric neutrinos oscillations can be stated with more confidence than the case for solar neutrino oscillations, because the atmospheric neutrino data spans over several decades in energy and distance which allows a better discrimination between the oscillation hypothesis and other flavour conversion mechanisms, which in general predict different dependence with energy and/or distance. In Fig. 5 I show the results of the phenomenological analysis from the Bari Group [24] on which they fit the atmospheric data with a conversion probability  $P_{\mu\tau} = \alpha \sin^2(\beta L E^n)$  which can parametrize several conversion mechanisms.  $n = -1$  corresponds to oscillations. Other mechanism can lead to different values of the index  $n$ , for instance, violation of Lorenz invariance, or violation of the equivalence principle imply  $n = 1$ , non-universal neutrino coupling to a space-time torsion field im-

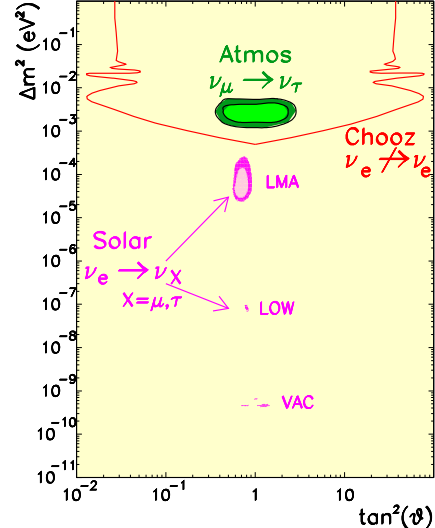


Figure 6. Pieces of the  $3\nu$  oscillation puzzle.

plies  $n = 0$ . The result of the fit shows that  $n = -1.03 \pm 0.31$  at 90%CL, clearly favouring the hypothesis of oscillations as conversion mechanism.

### 2.3. Three-Neutrino Oscillations

So far I have discussed the evidence for neutrino masses and mixings from solar and atmospheric data as usually formulated in the two-neutrino oscillation scenario. In Fig. 6 I show the summary of the allowed regions and channels from solar and atmospheric data together with the bounds from the CHOOZ reactor experiment. The minimum joint description of these data requires that all three known neutrinos take part in the oscillations.

The mixing parameters are encoded in the  $3 \times 3$  lepton mixing matrix which can be conveniently parametrized in the standard form

$$U = \begin{pmatrix} 1 & 0 & 0 \\ 0 & c_{23} & s_{23} \\ 0 & -s_{23} & c_{23} \end{pmatrix} \times \begin{pmatrix} c_{13} & 0 & s_{13} e^{i\delta} \\ 0 & 1 & 0 \\ -s_{13} e^{-i\delta} & 0 & c_{13} \end{pmatrix} \times \begin{pmatrix} c_{21} & s_{12} & 0 \\ -s_{12} & c_{12} & 0 \\ 0 & 0 & 1 \end{pmatrix}$$

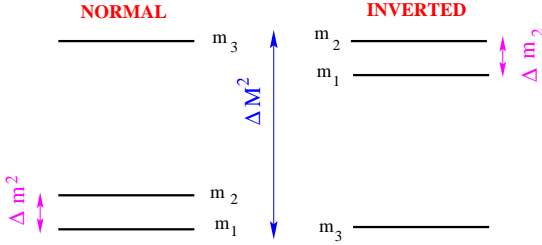


Figure 7. Mass schemes for  $3 \nu$  oscillations

where  $c_{ij} \equiv \cos \theta_{ij}$  and  $s_{ij} \equiv \sin \theta_{ij}$ . Notice that, since the two Majorana phases do not affect neutrino oscillations, they are not included in the expression above. The angles  $\theta_{ij}$  can be taken without loss of generality to lie in the first quadrant,  $\theta_{ij} \in [0, \pi/2]$ .

There are two possible mass orderings which, without any loss of generality can be chosen to be as shown in Fig. 7. The direct scheme is naturally related to hierarchical masses,  $m_1 \ll m_2 \ll m_3$ , for which  $m_2 \simeq \sqrt{\Delta m_{21}^2}$  and  $m_3 \simeq \sqrt{\Delta m_{32}^2}$ . On the other hand, the inverted scheme implies that  $m_3 < m_1 \simeq m_2$ . In both cases neutrinos can have quasi-degenerate masses,  $m_1 \simeq m_2 \simeq m_3 \gg \Delta m_{21}^2, |\Delta m_{32}^2|$ . The two orderings are often referred to in terms of the sign( $\Delta m_{31}^2$ ).

In total the three-neutrino oscillation analysis involves seven parameters: 2 mass differences, 3 mixing angles, the CP phase and the sign( $\Delta m_{31}^2$ ). Generic three-neutrino oscillation effects are:

- Coupled oscillations with two different oscillation lengths,
- CP violating effects,
- Difference between Normal and Inverted schemes

The strength of these effects is controlled by the values of the ratio of mass differences  $\Delta m^2/\Delta M^2$ , the mixing angle  $\theta_{13}$  and the CP phase  $\delta$ .

For solar and atmospheric oscillations, the required mass differences satisfy

$$\Delta m_{\odot}^2 = \Delta m^2 \ll \Delta M^2 = \Delta m_{\text{atm}}^2. \quad (11)$$

Under this condition, the joint three-neutrino analysis simplifies and

- For solar neutrinos the oscillations with the atmospheric oscillation length are averaged out and

the survival probability takes the form:

$$P_{ee,MSW}^{3\nu} = \sin^4 \theta_{13} + \cos^4 \theta_{13} P_{ee,MSW}^{2\nu} \quad (12)$$

where  $P_{ee,MSW}^{2\nu}$  is obtained with the modified sun density  $N_e \rightarrow \cos^2 \theta_{13} N_e$ . So the analyses of solar data constrain three of the seven parameters:  $\Delta m_{21}^2, \theta_{12}$  and  $\theta_{13}$ . The effect of  $\theta_{13}$  is to decrease the energy dependence of the solar survival probability.

– For atmospheric neutrinos, the solar wavelength is too long and the corresponding oscillating phase is negligible. As a consequence the atmospheric data analysis restricts  $\Delta m_{31}^2 \simeq \Delta m_{32}^2, \theta_{23}$  and  $\theta_{13}$ , the latter being the only parameter common to both solar and atmospheric neutrino oscillations and which may potentially allow for some mutual influence. The effect of  $\theta_{13}$  is to add a  $\nu_\mu \rightarrow \nu_e$  contribution to the atmospheric oscillations.

– At reactor experiments the solar wavelength is unobservable if  $\Delta m^2 < 8 \times 10^{-4}$  eV<sup>2</sup> and the relevant survival probability oscillates with wavelength determined by  $\Delta m_{31}^2$  and amplitude determined by  $\theta_{13}$ .

CP is unobservable in this approximation. There is, in principle some dependence on the Normal versus Inverted orderings due to matter effects in the Earth for atmospheric neutrinos, controlled by the mixing angle  $\theta_{13}$ . In Fig. 8 I plot the results of the analysis of solar, atmospheric and reactor data on the allowed values of  $\theta_{13}$ . The figure illustrates, that, at present, all data independently favours  $\theta_{13} = 0$ : the solar data exhibit energy dependence, the atmospheric data give no evidence for  $\nu_e$  oscillation, and, most important, reactor data exclude  $\bar{\nu}_e$ -disappearance at the atmospheric wavelength. The combined analysis results in a limit  $\sin^2 \theta_{13} \leq 0.06$  at  $3\sigma$  [23,26]. Within this limit the difference between Normal and Inverted orderings in atmospheric neutrino data is below present experimental sensitivity.

These results can be translated into our present knowledge of the moduli of the mixing matrix  $U$ :

$$|U| = \begin{pmatrix} 0.73 - 0.89 & 0.45 - 0.66 & < 0.24 \\ 0.23 - 0.66 & 0.24 - 0.75 & 0.52 - 0.87 \\ 0.06 - 0.57 & 0.40 - 0.82 & 0.48 - 0.85 \end{pmatrix} \quad (13)$$

which presents a structure

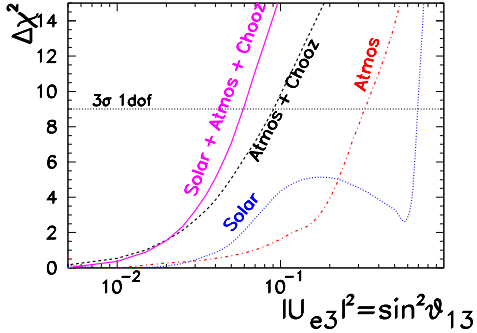


Figure 8. Dependence of  $\Delta\chi^2$  on  $\sin^2\theta_{13}$  in the analysis of the atmospheric, solar and CHOOZ neutrino data. The dotted horizontal line corresponds to the  $3\sigma$  limit for a single parameter.

$$|U| \simeq \begin{pmatrix} \frac{1}{\sqrt{2}}(1 + \mathcal{O}(\lambda)) & \frac{1}{\sqrt{2}}(1 - \mathcal{O}(\lambda)) & \epsilon \\ -\frac{1}{2}(1 - \mathcal{O}(\lambda) + \epsilon) & \frac{1}{2}(1 + \mathcal{O}(\lambda) - \epsilon) & \frac{1}{\sqrt{2}} \\ \frac{1}{2}(1 - \mathcal{O}(\lambda) - \epsilon) & -\frac{1}{2}(1 + \mathcal{O}(\lambda) - \epsilon) & \frac{1}{\sqrt{2}} \end{pmatrix}$$

with  $\lambda \sim 0.2$  and  $\epsilon < 0.25$ . This structure is very different from that of the quark sector

$$|U_{\text{CKM}}| \simeq \begin{pmatrix} 1 & \mathcal{O}(\lambda) & \mathcal{O}(\lambda^3) \\ \mathcal{O}(\lambda) & 1 & \mathcal{O}(\lambda^2) \\ \mathcal{O}(\lambda^3) & \mathcal{O}(\lambda^2) & 1 \end{pmatrix}$$

A good fraction of the papers of the last two years in Fig. 1 is devoted to find theoretical viable models *explaining* (or more accurately *accommodating*) this fact.

#### 2.4. LSND and Sterile Neutrinos

Together with the results from the solar and atmospheric neutrino experiments we have one more piece of evidence pointing out toward the existence of neutrino masses and mixing: the LSND results which finds evidence of  $\bar{\nu}_\mu \rightarrow \bar{\nu}_e$  with  $\Delta m^2 \geq 0.1 \text{ eV}^2$  (see Fig. 15). All data can be accommodated in a single neutrino oscillation framework only if there are at least three different scales of neutrino mass-squared differences which requires the existence of a fourth light neutrino. The measurement of the decay width of the  $Z^0$  boson into neutrinos makes the existence of three, and only three, light active neutrinos an experimental fact. Therefore, the fourth neutrino must

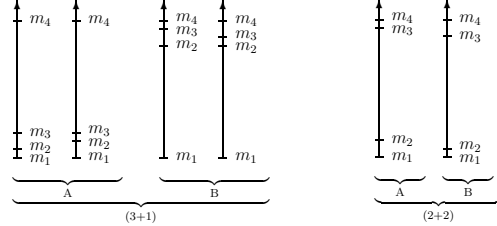


Figure 9. The six types of 4-neutrino mass spectra.

not couple to the standard electroweak current, that is, it must be sterile.

One of the most important issues in the context of four-neutrino scenarios is the four-neutrino mass spectrum. There are six possible four-neutrino schemes, shown in Fig. 9, that can accommodate the results from solar and atmospheric neutrino experiments as well as the LSND result. They can be divided in two classes: (3+1) and (2+2). In the (3+1) schemes, there is a group of three close-by neutrino masses that is separated from the fourth one by a gap of the order of  $1 \text{ eV}^2$ , which is responsible for the SBL oscillations observed in the LSND experiment. In (2+2) schemes, there are two pairs of close masses separated by the LSND gap. The main difference between these two classes is the following: if a (2+2)-spectrum is realized in nature, the transition into the sterile neutrino is a solution of either the solar or the atmospheric neutrino problem, or the sterile neutrino takes part in both, whereas with a (3+1)-spectrum the sterile neutrino could be only slightly mixed with the active ones and mainly provide a description of the LSND result.

The phenomenological situation at present is that none of the four-neutrino scenarios are favoured by the data as it was reviewed in the talk by Carlo Giunti [27] in the neutrino session. In brief (3+1)-spectra are disfavoured by the incompatibility between the LSND signal and the present constraints from short baseline laboratory experiments, while (2+2)-spectra are disfavoured by the existing constraints from the sterile oscil-

lations in solar and atmospheric data.

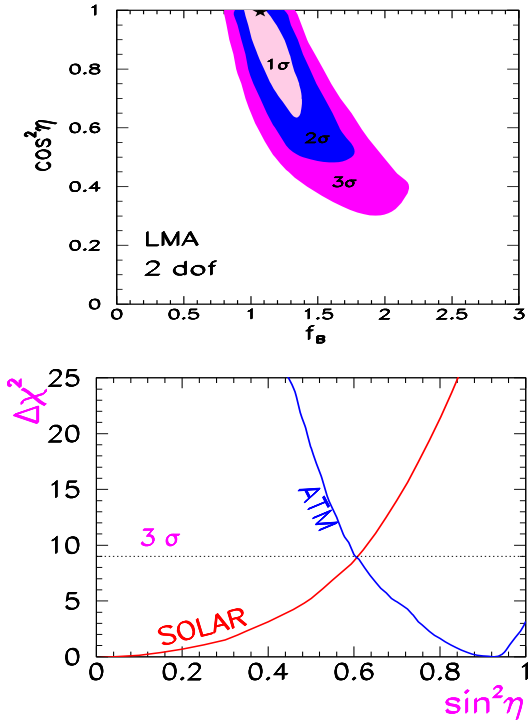


Figure 10. *Upper*: Constraint on the active-sterile admixture in solar neutrino oscillations versus the  ${}^8\text{B}$  neutrino flux enhancement factor. *Lower*: Present status of the bounds on the active-sterile admixture from solar (from Ref. [29]) and atmospheric (from Ref. [30]) neutrino data in (2+2)-models.

In this respect it has been recently pointed out that the existing constraint on the sterile admixture in the solar neutrino oscillations can be relaxed if the  ${}^8\text{B}$  neutrino flux is allowed to be larger than in the SSM by a factor  $f_B$  [28,29]. The analysis is performed in the context of solar conversion  $\nu_e \rightarrow \nu_x$ , where  $\nu_x = \cos \eta \nu_a + \sin \eta \nu_s$ . In Fig. 10 I show the presently allowed range of  $\eta$  as a function of  $f_B$ . The obtained upper bound on  $\sin^2 \eta$  from this most general solar analysis has to be compared with the corresponding lower bound

from the analysis of atmospheric data. In Fig. 10 I show the corresponding comparison (the curve for the atmospheric data is taken from Ref. [30]).

Alternative explanations to the LSND observation include the possibility of CPT violation [31] which would imply that the mass differences and mixing among neutrinos would be different from the ones for antineutrinos, or the possibility of lepton number violation in  $\mu$  decay:  $\mu^+ \rightarrow e^+ \bar{\nu}_e \bar{\nu}_i$  [32]. Again, we find ourselves in the privileged situation of having experiments running which will be able to test these scenarios. For example an imminent test of CPT will be the comparison of the observation in KamLAND of  $\bar{\nu}_e$  disappearance versus solar  $\nu_e$  disappearance. Also, at present, MiniBooNE [8] is running in the neutrino mode searching for  $\nu_\mu \rightarrow \nu_e$  to be compared with the antineutrino signal in LSND. Thus an oscillation signal at KamLAND or MiniBooNE will put serious constraints on CPT violation for  $\nu$ 's. Further precision tests can be performed at future facilities such as  $\nu$  factories [33].

### 3. Implications

#### 3.1. The Need of New Physics

The SM is based on the gauge symmetry  $SU(3)_C \times SU(2)_L \times U(1)_Y$  spontaneously broken to  $SU(3)_C \times U(1)_{\text{EM}}$  by the the vacuum expectations value (VEV),  $v$ , of the a Higgs doublet field  $\phi$ . The SM contains three fermion generations which reside in chiral representations of the gauge group. Right-handed fields are included for charged fermions as they are needed to build the electromagnetic and strong currents. No right-handed neutrino is included in the model since neutrinos are neutral.

In the SM, fermion masses arise from the Yukawa interactions,

$$-\mathcal{L}_{\text{Yukawa}} = Y_{ij}^d \overline{Q}_{Li} \phi D_{Rj} + Y_{ij}^u \overline{Q}_{Li} \tilde{\phi} U_{Rj} + Y_{ij}^\ell \overline{L}_{Li} \phi E_{Rj} + \text{h.c.}, \quad (14)$$

(where  $\tilde{\phi} = i\tau_2 \phi^*$ ) after spontaneous symmetry breaking. The Yukawa interactions of Eq. (14) lead to charged fermion masses

$$m_{ij}^f = Y_{ij}^f \frac{v}{\sqrt{2}} \quad (15)$$

but leave the neutrinos massless. No Yukawa interaction can be written that would give mass to the neutrino because no right-handed neutrino field exists in the model.

One could think that neutrino masses would arise from loop corrections if these corrections induced effective terms

$$\frac{Y_{ij}^\nu}{v} \left( \bar{L}_{Li} \tilde{\phi} \right) \left( \tilde{\phi}^T L_{Lj}^C \right) + \text{h.c.}, \quad (16)$$

( $L_{Lj}^C = C \bar{L}_{Lj}^T$ ). This, however, cannot happen, as can be easily understood by examining the accidental symmetries of the Standard Model. Within the SM the following accidental global symmetry arises:

$$G_{\text{SM}}^{\text{global}} = U(1)_B \times U(1)_e \times U(1)_\mu \times U(1)_\tau. \quad (17)$$

Here  $U(1)_B$  is the baryon number symmetry, and  $U(1)_{e,\mu,\tau}$  are the three lepton flavor symmetries, with total lepton number given by  $L = L_e + L_\mu + L_\tau$ . Terms of the form (16) violate  $G_{\text{SM}}^{\text{global}}$  and therefore cannot be induced by loop corrections. Furthermore, the  $U(1)_{B-L}$  subgroup of  $G_{\text{SM}}^{\text{global}}$  is non-anomalous. Terms of the form (16) have  $B-L = -2$  and therefore cannot be induced even by non-perturbative corrections.

It follows that the SM predicts that neutrinos are precisely massless. Consequently, there is neither mixing nor CP violation in the leptonic sector. Thus the simplest and most straightforward lesson of the evidence for neutrino masses is also the most striking one: *there is new physics beyond the SM*. This is the first experimental result that is inconsistent with the SM.

### 3.2. The Scale of New Physics

There are many good reasons to think that the SM is not a complete picture of Nature and some new physics (NP) is expected to appear at higher energies. In this case the SM is an effective low energy theory valid up to the scale  $\Lambda_{\text{NP}}$  which characterizes the NP. In this approach, the gauge group, the fermionic spectrum, and the pattern of spontaneous symmetry breaking are still valid ingredients to describe Nature at energies  $E \ll \Lambda_{\text{NP}}$ . The difference between the SM as a complete description of Nature and as a low energy effective theory is that in the latter case we

must consider also non-renormalizable ( $\text{dim} > 4$ ) terms whose effect will be suppressed by powers  $1/\Lambda_{\text{NP}}^{\text{dim}-4}$ . In this approach the largest effects at low energy are expected to come from  $\text{dim}=5$  operators

There is a single set of dimension-five terms that is made of SM fields and is consistent with the gauge symmetry given by

$$\mathcal{O}_5 = \frac{Z_{ij}^\nu}{2\Lambda_{\text{NP}}} \left( \bar{L}_{Li} \tilde{\phi} \right) \left( \tilde{\phi}^T L_{Lj}^C \right) + \text{h.c.}, \quad (18)$$

which violates total lepton number by two units and leads, upon spontaneous symmetry breaking, to neutrino masses:

$$(M_\nu)_{ij} = \frac{Z_{ij}^\nu}{2} \frac{v^2}{\Lambda_{\text{NP}}}. \quad (19)$$

This is a Majorana mass term.

Eq. (19) arises in a generic extension of the SM which means that neutrino masses are very likely to appear if there is NP. Furthermore comparing Eq. (19) and Eq. (15) we find that the scale of neutrino masses is suppressed by  $v/\Lambda_{\text{NP}}$  when compared to the scale of charged fermion masses providing an explanation not only for the existence of neutrino masses but also for their smallness. Finally, Eq. (19) breaks not only total lepton number but also the lepton flavor symmetry  $U(1)_e \times U(1)_\mu \times U(1)_\tau$ . Therefore we should expect lepton mixing and CP violation.

Given the relation (19),  $m_\nu \sim v^2/\Lambda_{\text{NP}}$ , it is straightforward to use measured neutrino masses to estimate the scale of NP that is relevant to their generation. In particular, if there is no quasi-degeneracy in the neutrino masses, the heaviest of the active neutrino masses can be estimated,

$$m_h = m_3 \sim \sqrt{\Delta m_{\text{atm}}^2} \approx 0.05 \text{ eV}. \quad (20)$$

(In the case of inverted hierarchy the implied scale is  $m_h = m_2 \sim \sqrt{|\Delta m_{\text{atm}}^2|} \approx 0.05 \text{ eV}$ ). It follows that the scale in the non-renormalizable term (18) is given by

$$\Lambda_{\text{NP}} \sim v^2/m_h \approx 10^{15} \text{ GeV}. \quad (21)$$

We should clarify two points regarding Eq. (21):

1. There could be some level of degeneracy between the neutrino masses that are relevant to the atmospheric neutrino oscillations. In such a case Eq. (20) is modified into a lower bound and, consequently, Eq. (21) becomes an upper bound on the scale of NP.

2. It could be that the  $Z_{ij}$  couplings of Eq. (18) are much smaller than one. In such a case, again, Eq. (21) becomes an upper bound on the scale of NP. On the other hand, in models of approximate flavor symmetries, there are relations between the structures of the charged lepton and neutrino mass matrices that give quite generically  $Z_{33} \geq m_\tau^2/v^2 \sim 10^{-4}$ . We conclude that the likely range of  $\Lambda_{\text{NP}}$  that is implied by the atmospheric neutrino results is given by

$$10^{11} \text{ GeV} \leq \Lambda_{\text{NP}} \leq 10^{15} \text{ GeV}. \quad (22)$$

The estimates (21) and (22) are very exciting. First, the upper bound on the scale of NP is well below the Planck scale. This means that there is a new scale in Nature which is intermediate between the two known scales, the Planck scale  $m_{\text{Pl}} \sim 10^{19}$  GeV and the electroweak breaking scale,  $v \sim 10^2$  GeV.

It is amusing to note in this regard that the solar neutrino problem does not necessarily imply such a new scale. If its solution is related to vacuum oscillations with  $\Delta m_{21}^2 \sim 10^{-10}$  eV<sup>2</sup>, it can be explained by  $\Lambda_{\text{NP}} \sim m_{\text{Pl}}$ . However, the favoured explanation for the solar neutrino deficit is the LMA solution which again points towards NP scale in the range of Eq. (22).

Second, the scale  $\Lambda_{\text{NP}} \sim 10^{15}$  GeV is intriguingly close to the scale of gauge coupling unification.

Of course, neutrinos could be conventional Dirac particles. In the minimal realization of this possibility, one must still extend the SM to add right-handed neutrinos and impose the conservation of total lepton number (since in the presence of right-handed neutrinos total lepton number is not an accidental symmetry) to prevent the right-handed neutrinos from acquiring a singlet Majorana mass term. In this scenario, neutrinos could acquire a mass like any other fermion of the Standard Model and no NP scale would be implied. We would be left in the darkness on the reason of

the smallness of the neutrino mass.

### 3.3. Reconstructing the Neutrino Mass Matrix

The best known scenario that leads to (18) is the *see-saw mechanism* [34]. Here one assumes the existence of heavy sterile neutrinos  $N_i$ . Such fermions have SM gauge invariant bare mass terms and Yukawa interactions :

$$-\mathcal{L}_{\text{NP}} = \frac{1}{2} M_{Nij} \overline{N}_i^c N_j + Y_{ij}^\nu \overline{L}_{Li} \tilde{\phi} N_j + \text{h.c.} \quad (23)$$

The resulting mass matrix in the basis  $\begin{pmatrix} \nu_{Li} \\ N_j \end{pmatrix}$  has the following form:

$$M_\nu = \begin{pmatrix} 0 & Y^\nu \frac{v}{\sqrt{2}} \\ (Y^\nu)^T \frac{v}{\sqrt{2}} & M_N \end{pmatrix}. \quad (24)$$

If the eigenvalues of  $M_N$  are all well above the electroweak breaking scale  $v$ , then the diagonalization of  $M_\nu$  leads to three light mass eigenstates and an effective low energy interaction of the form (18). In particular, the scale  $\Lambda_{\text{NP}}$  is identified with the mass scale of the heavy sterile neutrinos, that is the typical scale of the eigenvalues of  $M_N$ . Two well-known examples of extensions of the SM that lead to a see-saw mechanism for neutrino masses are SO(10) GUTs and left-right symmetry.

One may notice that even in this particularly simple form of NP,  $\mathcal{L}_{\text{NP}}$  contains 18 parameters which we would need to know in order to fully determine the dynamics of the NP. However the effective low energy operator  $\mathcal{O}_5$  contains only 9 parameters which we can hope to measure at the low energy experiments. This simple parameter counting illustrates the limitation of the “bottom-up” approach in deriving model independent implications of the presently observed neutrino masses and mixing.

Alternatively one can go “top-down” by studying the low energy effective neutrino masses and mixing induced by specific high energy models [26]. For example, in his talk, Q. Shafi [35] discussed the possibility of accommodating the present neutrino data in the framework of theories with warped extra dimensions. Unfortunately the number of possible models is overwhelming and impossible to review in this talk.

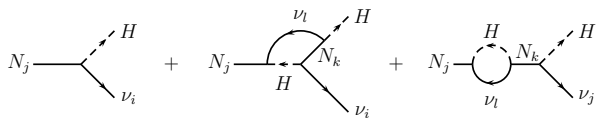


Figure 11. The tree-level and one-loop diagrams of right-handed neutrino decay into leptons and Higgs.

An intermediate approach is the attempt to classify different forms of NP in terms of the characteristic texture of the induced low energy neutrino mass matrices [36]. The main goal is to identify generic predictions which, with more data at hand, will be able to discriminate among the different textures. In general, depending on the specific texture, different relations between the mass differences and the mixing angles are expected. For example relations between the value of  $\theta_{13}$  and the ratio of the masses, and different rate for neutrinoless double beta decay, which could be tested once the parameters are known to good enough precision.

The bottom line is that in order to advance further in this direction we need more (and more precise) data. As we will see even at the end of the program of the presently approved experiments we will still be far from reaching this goal.

### 3.4. A Side Effect: Leptogenesis

Finally I would like to comment a possible *side effect*<sup>2</sup> of neutrino masses which is that they may help us to explain “how we are here”. What I mean with this, is the explanation of the origin of the cosmic matter-antimatter asymmetry via leptogenesis [37]. From the Big-Bang Nucleosynthesis, we know that there is only a tiny asymmetry in the baryon number,  $n_B/n_\gamma \approx 5 \times 10^{-10}$ . Leptogenesis [37] is the possible origin of such a small asymmetry related to neutrino physics.

In a possible realization of leptogenesis,  $L \neq 0$  is generated in the Early Universe by the decay of one of the heavy right-handed neutrinos of the see-saw mechanism, with a direct CP violation.

Due to the interference between the tree-level and one-loop diagrams shown in Fig. 11 the decay rates of the right-handed neutrino into leptons and anti-leptons are different. In order to generate a lepton asymmetry the decay must be out of equilibrium ( $\Gamma_{\nu_R} \ll$  Universe expansion rate). Sphaleron processes transform the lepton asymmetry into a baryon asymmetry and below the electroweak phase transition a net baryon asymmetry is generated  $\Delta B \simeq -\frac{\Delta L}{2}$  (the exact coefficient relating  $\Delta B$  to  $\Delta L$  is model dependent.)

The details of the leptogenesis scenario are model dependent and much work has been done in the framework of specific neutrino models (see, for example, the talk by Xing [39]). In particular, it has been shown that a right-handed neutrino of about  $10^{10}$  GeV can account for the cosmic baryon asymmetry from its out-of-equilibrium decay [38].

## 4. Future

### 4.1. KamLAND and Borexino

Our present understanding of the solar neutrino oscillation is being tested in the KamLAND experiment which is currently in operation in the Kamioka mine in Japan. This underground site is conveniently located at a distance of 150-210 km from several Japanese nuclear power stations. The measurement of the flux and energy spectrum of the  $\bar{\nu}_e$ 's emitted by these reactors will provide a test to the LMA solution of the solar neutrino anomaly [4]. In Fig. 12 I show the expected distortion on the energy spectrum in the presence of oscillations. After two or three years of data taking, KamLAND should be capable of either excluding the entire LMA region or, not only establishing  $\nu_e \leftrightarrow \nu_{\text{other}}$  oscillations, but also measuring the LMA oscillation parameters with unprecedented precision [41,40,29] provided that  $\Delta m^2 \leq \text{few} 10^{-4} \text{ eV}^2$ . KamLAND is expected to announce their first results this year.

If LMA is confirmed, CP violation may be observable at future long-baseline (LBL) experiments. Also KamLAND will provide us, as data accumulate, with a firm determination of the corresponding oscillation parameters. With this at hand, the future solar  $\nu$  experiments will be able

<sup>2</sup>I call it side effect because it is not guaranteed to happen.

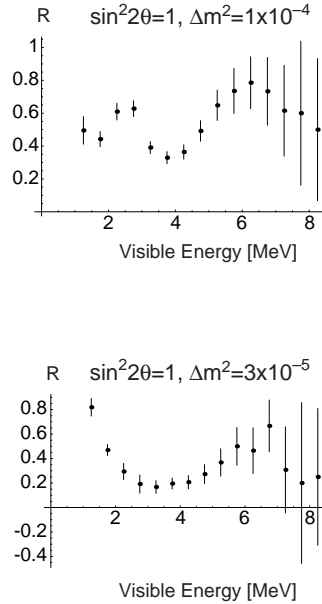


Figure 12. Predicted distortion in the energy spectrum of KamLAND in the presence of oscillations, from Ref. [41].

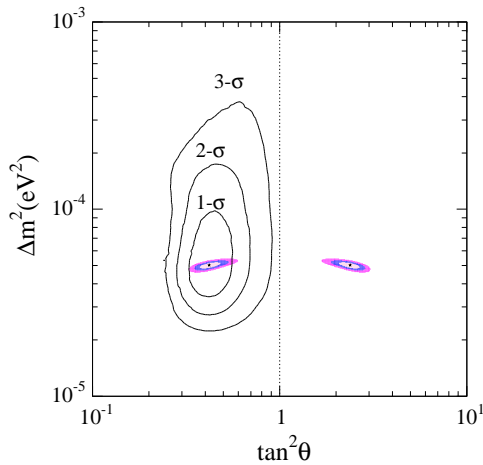


Figure 13. Expected reconstructed regions if KamLAND observes a signal corresponding to the present best fit point of the LMA region. From Ref. [29].

to return to their original goal of testing solar physics.

If KamLAND does not confirm LMA, the next most relevant results will come from Borexino [42]. The Borexino experiment is designed to detect low-energy solar neutrinos in real-time through the observation of the ES process  $\nu_a + e^- \rightarrow \nu_a + e^-$ . The energy threshold for the recoil electrons is 250 keV. The largest contribution to their expected event rate is from neutrinos of the  ${}^7\text{Be}$  line. Due to the lower energy threshold, Borexino is sensitive to matter effects in the Earth in the LOW region. And because  ${}^7\text{Be}$  neutrinos are almost monoenergetic, it is also very sensitive to seasonal variations associated with VAC oscillations.

#### 4.2. Long Baseline Experiments

$\nu_\mu$  oscillations with  $\Delta m_{\text{atm}}^2$  are being probed and will be further tested using accelerator beams at LBL experiments. In these experiments the intense neutrino beam from an accelerator is aimed at a detector located underground at a distance of several hundred kilometers. At present there are three such projects approved: K2K [6] which runs with a baseline of about 235 km from KEK to SK, MINOS [9] under construction with a baseline of 730 km from Fermilab to the Soudan mine where the detector will be placed, and OPERA [43] under construction with a baseline of 730 km from CERN to Gran Sasso.

The first results from K2K seem to confirm the atmospheric oscillations but statistically they are still not very significant. In the near future K2K will accumulate more data enabling it to confirm the atmospheric neutrino oscillation. Furthermore, combining the K2K and atmospheric neutrino data will lead to a better determination of the mass and mixing parameters.

In a longer time scale, the results from MINOS will provide more accurate determination of these parameters as shown in Fig. 14. OPERA is designed to observe the  $\nu_\tau$  appearance. Both MINOS and OPERA have certain sensitivity to  $\theta_{13}$  although by how much they will be ultimately able to improve the present bound is still undetermined.

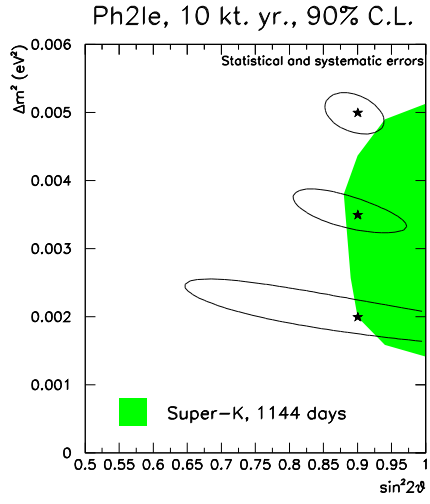


Figure 14. Expected reconstruction of the oscillation parameters in Minos. See Ref. [9] for details.

#### 4.3. MiniBOONE

The MiniBooNE experiment [8], will be able to confirm or disprove the LSND oscillation signal within the next two years (see Fig. 15). Should the signal be confirmed as well as the solar signal in KamLAND and the atmospheric in LBL experiments, we will face the challenging situation of not having a successful “minimal” phenomenological description at low-energy of the leptonic mixing.

#### 4.4. Neutrino Mass Scale

Oscillation experiments provide information on  $\Delta m_{ij}^2$ , and on the leptonic mixing angles,  $U_{ij}$ . But they are insensitive to the absolute mass scale for the neutrinos. Of course, the results of an oscillation experiment do provide a lower bound on the heavier mass in  $\Delta m_{ij}^2$ ,  $|m_i| \geq \sqrt{\Delta m_{ij}^2}$  for  $\Delta m_{ij}^2 > 0$ . But there is no upper bound on this mass. In particular, the corresponding neutrinos could be approximately degenerate at a mass scale that is much higher than  $\sqrt{\Delta m_{ij}^2}$ . Moreover, there is neither upper nor lower bound on the lighter mass  $m_j$ .

Information on the neutrino masses, rather than mass differences, can be extracted from kinematic studies of reactions in which a neutrino or

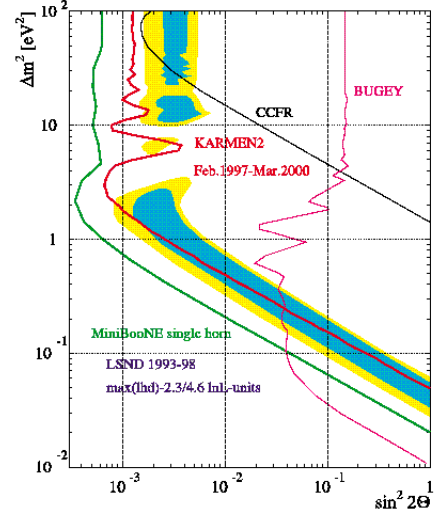


Figure 15. Allowed regions (at 90 and 99 % CL) for  $\nu_e \rightarrow \nu_\mu$  oscillations from the LSND experiment compared with the exclusion regions (at 90% CL) from KARMEN2 and other experiments. The 90 % CL expected sensitivity curve for MiniBooNE is also shown.

an anti-neutrino is involved. In the presence of mixing the most relevant constraint comes from Tritium beta decay  ${}^3\text{H} \rightarrow {}^3\text{He} + e^- + \bar{\nu}_e$  which, within the present and expected experimental accuracy, can limit the combination

$$m_\beta = \sum_i m_i |U_{ei}|^2 \quad (25)$$

The present bound is  $m_\beta \leq 2.2$  eV at 95 % CL [44]. A new experimental project, KATRIN, is under consideration with an estimated sensitivity limit:  $m_\beta \sim 0.3$  eV [1].

Direct information on neutrino masses can also be obtained from neutrinoless double beta decay  $(A, Z) \rightarrow (A, Z + 2) + e^- + e^-$ . The rate of this process is proportional to the *effective Majorana mass of  $\nu_e$* ,

$$m_{ee} = \left| \sum_i m_i U_{ei}^2 \right| \quad (26)$$

which, unlike Eq. (25), depends also on the three CP violating phases. Notice that in order to induce the  $2\beta 0\nu$  decay,  $\nu$ 's must Majorana particles.

The present strongest bound from  $2\beta0\nu$ -decay is  $m_{ee} < 0.34$  eV at 90 % CL [45]. Taking into account systematic errors related to nuclear matrix elements, the bound may be weaker by a factor of about 3. A sensitivity of  $m_{ee} \sim 0.1$  eV is expected to be reached by the currently running NEMO3 experiment, while a series of new experiments (CUORE, EXO, GENIUS) is planned with sensitivity of up to  $m_{ee} \sim 0.01$  eV [1].

The knowledge of  $m_{ee}$  can provide information on the mass and mixing parameters that is independent of the  $\Delta m_{ij}^2$ 's. However, to infer the values of neutrino masses, additional assumptions are required. In particular, the mixing elements are complex and may lead to strong cancellation,  $m_{ee} \ll m_1$ . Yet, the combination of results from  $2\beta0\nu$  decays and Tritium beta decay can test and, in some cases, determine the mass parameters of given schemes of neutrino masses [46] provided that the nuclear matrix elements are known to good enough precision.

#### 4.5. Future Facilities

At the end of the presently approved neutrino experiments, many questions will still remain open. Even in the scenario in which Mini-BooNE does not confirm the LSND signal, and we can live with oscillations among the three known neutrinos, we will still be ignorant about: (i) the value of  $\theta_{13}$ , (ii) the  $\text{sign}(\Delta m_{13}^2)$ , and (iii) the possibility of CP violation in the lepton sector.

To measure these parameters, the following is required of future experiments:

- (i) To measure  $\theta_{13}$ : Very intense beam with low background
- (ii) To discriminate Normal/Inverted: Matter effects which implies very long baseline.
- (iii) To detect CP violation: LMA must be confirmed and  $\theta_{13}$  should be not too small. One must have intense beams with exchangeable initial state ( $\nu/\bar{\nu}$ ).

New facilities and experiments are being proposed which can realize some of all of these conditions. In particular, for future neutrino oscillation experiments two type of facilities are being proposed: conventional neutrino superbeams [48,7] (conventional meaning from the decay of pions generated from a proton beam dump) with a de-

tector either on or off axis, and neutrino beams from muon decay in muon storage rings [49]. As an illustration of the possible reach of these facilities I show in Fig. 16 the required values of  $\Delta m_{21}^2$  and mixing angle  $\theta_{13}$  which would allow to measure a maximal CP violation phase at different type of neutrino beams (from the CERN working group on Super Beams [50]) See Ref. [1]

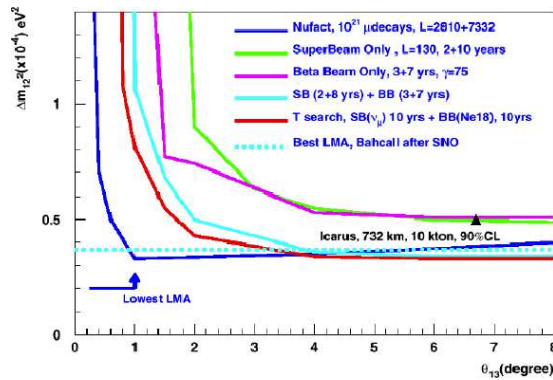


Figure 16. Required values of  $\Delta m_{21}^2$  and mixing angle  $\theta_{13}$  which would allow to measure a maximal CP violation phase at different types of neutrino beams and baselines.

for a more exhaustive comparison of the expected reach of these proposals.

In general, the independent determination of these missing pieces of the puzzle at these facilities becomes challenging because in the relevant oscillation probabilities there appear three independent two-fold parameter degeneracies ( $\delta_{CP}, \theta_{13}$ ),  $\text{sign}(\Delta m_{31}^2)$  and  $(\theta_{23}, \pi/2 - \theta_{23})$ . The phenomenological efforts in this front concentrate on the study of how the combination of data from experiments performed at different baselines and different beam types can help in resolving these degeneracies [47].

#### 5. Conclusions

Neutrino physics is a very exciting field which is at the moment experimentally driven. An enormous experimental effort has been devoted in the last years to prove beyond doubt the presence of neutrino masses and mixing. In the last year, the

SNO experiment has provided model independent evidence of flavour conversion of solar  $\nu'_e$ 's at more than  $5\sigma$  CL. SuperKamiokande has accumulated more and more data on the disappearance of atmospheric  $\nu_\mu$ 's resulting into a high confidence of the  $L/E$  dependence of their survival probability.

At present these signals are being probed and will be further tested with “human-made” neutrino beams from reactor and accelerators. For solar  $\nu$ 's KamLAND should give us a definite answer on the LMA solution to the solar neutrino problem and provide us with a precise determination of the corresponding oscillation parameters. The present K2K data seem to confirm the atmospheric neutrino oscillation within the limited statistics. The experiments should soon recover from the accident in SuperKamiokande, and with additional data will provide a more meaningful test of the oscillation. In the near future MINOS will measure the oscillation parameters with precision. Within the next two years MiniBooNE will definitively test the LSND signal.

Neutrino masses imply physics beyond the Standard Model and they most probably suggest a NP scale close to GUT scale. The implied existence of heavy, SM-singlet neutrinos opens up the possibility of leptogenesis as the mechanism for generation of the baryon asymmetry.

Determining the parameters of the neutrino mass matrix will provide fundamental information to understand the dynamics at the new physics scale. However even at the end of the existing neutrino programs, we will still be far from reaching this goal. Further advance requires a new generation of neutrino experiments.

### Acknowledgements

I want to give special thanks to J.N. Bahcall, J.J. Gomez-Cadenas, P. Hernandez, M. Maltoni, A. Marrone and C. Peña-Garay, for their help in the preparation of my talk. This work is supported by the MC fellowship HPMF-CT-2000-00516 and by the Spanish DGICYT grant FPA2001-3031.

### REFERENCES

1. David Wark in these proceedings.
2. Scott Oser in these proceedings.
3. Mark R. Vagins in these proceedings.
4. Tadao Mitsui in these proceedings.
5. Christopher Mauger in these proceedings.
6. Yoshinari Hayato in these proceedings.
7. Y. Itow in these proceedings.
8. Andrew Bazarko in these proceedings
9. J. Urheim in these proceedings.
10. Z. Maki, M. Nakagawa, and S. Sakata, *Prog. Theor. Phys.* **28**, 870 (1962).
11. Kobayashi, M., and T. Maskawa,, *Prog. Theor. Phys.* **49**, 652 (1973).
12. L. Wolfenstein, *Phys. Rev. D* **17**, 2369 (1978); S.P. Mikheyev, and A.Y. Smirnov, *Yad. Fiz.* **42**, 1441 (1985) [*Sov. J. Nucl. Phys.* **42**, 913].
13. A. de Gouvea, A. Friedland and H. Murayama, *Phys. Lett. B* **490**, 125 (2000); M. C. Gonzalez-Garcia, C. Peña-Garay, *Phys. Rev. D* **62**, 031301 (2000); G. L. Fogli, E. Lisi, A. Marrone and G. Scioscia, *Phys. Rev. D* **59**, 033001 (1999); C. Giunti, M. C. Gonzalez-Garcia, C. Peña-Garay, *Phys. Rev. D* **62**, 013005 (2000).
14. J.N. Bahcall, H.M. Pinsonneault, and S. Basu, *Astrophys. J.* **555**, 990 (2001).
15. SNO coll., *nucl-ex/0204009*; Barger *et al.*, *hep-ph/0204253*; Bandyopadhyay *et al*, *hep-ph/0204286*; Bahcall *et al*, *hep-ph/0204314*; Creminelli *et al*, *hep-ph/0102234*; Aliani *et al* *hep-ph/0205053*; de Holanda, Smirnov, *hep-ph/0205241*; Strumia *et al*, *hep-ph/0205262*; Fogli *et al*, *hep-ph/0206162*; Maltoni *et al*,*hep-ph/0207227*.
16. J.N. Bahcall, M.C. Gonzalez-Garcia, C. Peña-Garay, *JHEP* **0207**, 054 (2002).
17. M.C. Gonzalez-Garcia, Osaka 2000, High energy physics, vol. 2 899-906, *hep-ph/0010136*
18. V. S. Berezinsky, M. Lissia, *hep-ph/0108108*; G. L. Fogli *et al.*, *hep-ph/0203138*; V. Barger, D. Marfatia, K. Whisnant, B. Wood, *hep-ph/0204253*.
19. C.S. Lim, W. J. Marciano, *Phys. Rev. D* **37** 1369 (1988); E. Kh Akhmedov, *Phys. Lett. B* **213**, 64 (1988).
20. E. K. Akhmedov, J. Pulido, *Phys. Lett.*

**B529**, 193 (2002); A. M. Gago, et al, Phys. Rev. **D65** 073012 (2002); O. G. Miranda et al., hep-ph/0108145; A. Friedland, A. Gruzinov, hep-ph/0202095; B. C. Chauhan, J. Pulido hep-ph/0206193; J. Barranco, O.G. Miranda, T.I. Rashba, V.B. Semikoz, J.W.F. Valle, hep-ph/0207326.

21. L. Wolfenstein, Phys. Rev. **D17** 2369 (1978)  
E. Roulet, Phys. Rev. **D44** R935 (1991); M. M. Guzzo, A. Masiero, S. T. Petcov, Phys. Lett. **B260**, 154 (1991).

22. Guzzo et al hep-ph/0112310; Gago et al hep-ph/0112060.

23. M. C. Gonzalez-Garcia and M. Maltoni, hep-ph/0202218.

24. Fogli, Lisi and Marrone, Phys. Rev. D **64**, 093005 (2001).

25. CHOOZ Collaboration, M. Apollonio et al., Phys. Lett. **B420**, 397 (1998).

26. M.C. Gonzalez-Garcia and Y. Nir, hep-ph/0202058, Rev. Mod. Phys, in press.

27. C. Giunti in these proceedings.

28. V. Barger, D. Marfatia, and K. Whisnant, Phys. Rev. Lett. **88**, 011302 (2002)

29. J. N. Bahcall, M. C. Gonzalez-Garcia and C. Pena-Garay, Phys. Rev. C **66**, 035802 (2002).

30. Maltoni, M., M.A. Tortola, T. Schwetz and J.W. Valle, 2002, hep-ph/0207227.

31. H. Murayama, and T. Yanagida, , Phys. Lett. B **520**, 263 (2001); S. Pakvasa, hep-ph/0110175; Barenboim et al., hep-ph/0108199; Skadghauge, hep-ph/0112189; A. Strumia, hep-ph/0201134.

32. K.S. Babu in these proceedings.

33. T. Ohlsson in these proceedings.

34. P. Ramond, CALT-68-709 (1979); M.P. Gell-Mann, P. Ramond and R. Slansky, 1979, in *Supergravity*, edited by P. van Nieuwenhuizen and D.Z. Freedman (North Holland); T. Yanagida, 1979, in *Proceedings of Workshop on Unified Theory and Baryon Number in the Universe*, edited by O. Sawada and A. Sugamoto (KEK); R.N. Mohapatra, and G. Senjanovic, 1980, Phys. Rev. Lett. **44**, 912.

35. Q. Shafi in these proceedings.

36. For a recent review see G. Altarelli and F. Feruglio, hep-ph/0206077, and references therein.

37. M. Fukugita and T. Yanagida, Phys. Lett. B **174**, 45 (1986).

38. See for example, W. Buchmuller, hep-ph/0107153. talk at Presented at 8th International Symposium on Particle Strings and Cosmology (PASCOS 2001), Chapel Hill, North Carolina, 10-15, 2001.

39. See Z. Xing in these proceedings.

40. V. D. Barger, D. Marfatia and B. P. Wood, Phys. Lett. B **498**, 53 (2001); A. de Gouv   and C. Pe  a-Garay, Phys. Rev. D **64**, 113011 (2001)

41. H. Murayama and A. Pierce, Phys. Rev. D **65**, 013012 (2002)

42. L. Oberauer, Nucl. Phys. Proc. Suppl. **77**, 48 (1999).

43. A.G. Cocco, et al., OPERA Coll., Nucl. Phys. Proc. Suppl. **85**, 125 (2000).

44. J. Bonn, et al., Nucl. Phys. Proc. Suppl. **91**, 273 (2001); V.M. Lobashev, et al., Nucl. Phys. Proc. Suppl. **91**, 280 (2001).

45. H.V. Klapdor-Kleingrothaus, H.V., Eur. Phys. J. A **12** 147 (2001).

46. F. Vissani, JHEP **9906**, 022 (1999); Y. Farzan, O. L. Peres and A. Y. Smirnov, Nucl. Phys. B **612**, 59 (2001); S.M. Bilenky, S.M., S. Pascoli and S. T. Petcov, Phys. Rev. D **64**, 053010 (2001); *ibid* 113003; S. Pascoli, and T.S. Petcov hep-ph/0205022.

47. V. Barger, D. Marfatia and K. Whisnant, Phys. Rev. D **65**, 073023 (2002); P. Huber, M. Lindner and W. Winter, hep-ph/0204352; J. Burguet-Castell, M. B. Gavela, J. J. Gomez-Cadenas, P. Hernandez and O. Mena, hep-ph/0207080.

48. B. Richter, hep-ph/0008222; V. D. Barger, S. Geer, R. Raja and K. Whisnant, Phys. Rev. D **63**, 113011 (2001); J. J. Gomez-Cadenas et al., hep-ph/0105297; Y. Itow, et al., hep-ex/0106019.

49. S. Geer, Phys. Rev. D **57** 6989 (1998). A. De Rujula, M. B. Gavela and P. Hernandez, Nucl. Phys. B **547**, 21 (1999); J. J. Gomez-Cadenas and D. A. Harris, FERMILAB-PUB-02-044-T.

50. M. Mezzetto and J.J. Gomez-Cadenas, private communication.